

Polar-optical phonon-limited transport in degenerate GaN-based quantum wells

D. R. Anderson,¹ N. A. Zakhleniuk,² M. Babiker,¹ B. K. Ridley,³ and C. R. Bennett¹

¹*Department of Physics, University of York, Heslington, York YO10 5DD, United Kingdom*

²*Marconi Caswell Technology, Caswell, Towcester, Northants NN12 8EQ, United Kingdom*

³*Department of Electronic Systems Engineering, University of Essex, Colchester CO4 3SQ, United Kingdom*

(Received 5 December 2000; published 5 June 2001)

A theory of polar-optical phonon-limited electron transport in GaN-based quantum wells is developed within the Boltzmann equation approach. The linearized Boltzmann equation is solved for a degenerate two-dimensional electron system using a ladder technique, enabling evaluations of the effective momentum relaxation time and the low-field electron mobility to be carried out. Variations of the effective momentum relaxation time with the well width, electron energy, lattice temperature, and electron density are explored in these heterostructures. The corresponding mobility is then evaluated and its variations with the well width, lattice temperature, and electron density displayed. Comparison is made, where appropriate, with the results emerging from the application of a low-energy approximation.

DOI: 10.1103/PhysRevB.63.245313

PACS number(s): 72.10.-d, 72.20.Dp, 72.80.Ey

I. INTRODUCTION

The current heightened interest in the optical and electronic properties of large band-gap semiconductors, particularly the III nitrides, is motivated by their potential for device applications and for operation at short wavelengths with sustained performance at high temperatures.¹ Although at present GaN and related compounds are not sufficiently pure to justify completely ignoring the influences of other scattering processes, particularly effects associated with impurities and dislocation mechanisms, the dominant scattering process in such materials at room temperature and above is still polar-optical phonon scattering.²

It is well known that in large band-gap quantum wells, the typical well depth can be in excess of 1 eV, which facilitates the buildup of confined electrons to high densities. The two-dimensional electron gases generated in this context are highly degenerate and remain so even at lattice temperatures well in excess of room temperature. Clearly any treatment of polar-optical phonon scattering effects and the associated electron transport under these conditions must take account of the strongly degenerate feature of the electron gas.

In this paper we consider electron transport in GaN/AlN and other GaN-based quantum wells, incorporating the degeneracy of the electron system. We concentrate on square quantum wells, which we assume have well-defined widths. This case should be distinguished from the situation in which the growth process leads to a layer structure with strong interface electric fields perpendicular to the layer planes. These fields are either strain-induced or, in the case of wurtzite GaN, are, in addition, also attributable to spontaneous polarization.³⁻⁵ The strong fields lead to deeper effective quantum wells at the interfaces and hence stronger carrier confinement. As a result, two-dimensional electron densities in excess of 10^{13} cm^{-2} build up and have indeed been observed in GaN heterostructures even in the absence of modulation doping.⁶⁻¹² Under such circumstances, however, the real shape of the quantum well is not square and it also depends on the electron density.

Here we seek to determine the solution of the Boltzmann

equation in the linear regime. We are mainly concerned with the mobility in the degenerate two-dimensional electron gas and will concentrate on the situation when there is only one electronic subband occupied since it is in this case that the quantum effects are largest. It is easy to see that the case when many subbands are occupied is close to the three-dimensional situation. The one-subband case is illustrated schematically in Fig. 1 in which the Fermi energy has been chosen to be smaller than the polar-optical (PO) phonon energy $\hbar\omega_{\text{LO}}$. This situation is realizable for GaN-based heterostructures, even at high densities, on account of the large magnitude of $\hbar\omega_{\text{LO}}$ (for GaN we have $\hbar\omega_{\text{LO}} \approx 92.8 \text{ meV}$). We also assume that the polar-optical phonons with which the electrons exchange energy are not affected by the heterostructure and so assume their bulk form. This is a reasonable approximation since we are interested in total scattering rates and thus may invoke the approximate sum rule applicable in this case, provided that the quantum wells are not too narrow.^{13,14} Our aim is to evaluate a momentum relaxation time and hence determine the mobility under the above-mentioned conditions and examine the variations of the results with the system parameters.

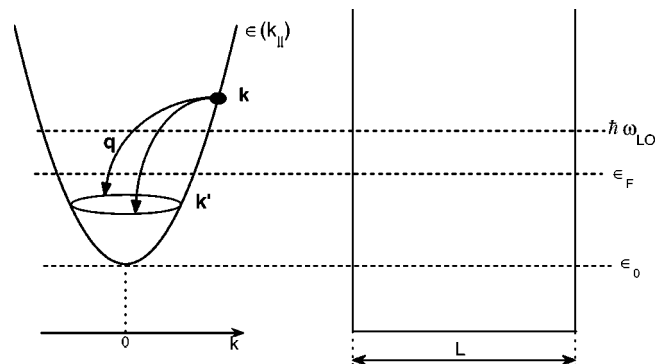


FIG. 1. A schematic drawing of the one-subband model showing the lowest quantum well subband. The relative positions of the Fermi energy and the optical phonon energy are also shown.

II. ELECTRON-PHONON INTERACTION IN QUANTUM WELLS

The system in question is a 2D electron gas confined in a GaN/AlN quantum well. We consider a square quantum well of width L and, for our purpose, it suffices to assume that the quantum well is infinitely deep, in which case the energy spectrum of the electrons with in-plane wave vector \mathbf{k}_{\parallel} in subband n is given by $\epsilon_n(\mathbf{k}_{\parallel}) = n^2 \epsilon_1 + \epsilon_{\mathbf{k}_{\parallel}}$ where $n = 1, 2, \dots$, $\epsilon_1 = \pi^2 \hbar^2 / 2m^* L^2$, and $\epsilon_{\mathbf{k}_{\parallel}} = \hbar^2 k_{\parallel}^2 / 2m^*$ with m^* the effective mass. The probability of transition from an electron state of in-plane wave vector \mathbf{k}_{\parallel} within the lowest subband $n=1$ to state \mathbf{k}'_{\parallel} within the same subband by emission (+) or absorption (-) of a PO phonon of wave vector $\mathbf{q} = (q_{\parallel}, q_z)$ is given by

$$W_{\mathbf{k}_{\parallel}, \mathbf{k}'_{\parallel}, \mathbf{q}}^{\pm} = \frac{\pi e^2 \omega_{\text{LO}}}{V_0 \epsilon_0} \left(\frac{1}{\epsilon_{\infty}} - \frac{1}{\epsilon_s} \right) \left\{ N + \frac{1}{2} \pm \frac{1}{2} \right\} \times \frac{|G(q_z)|^2}{q_{\parallel}^2 + q_z^2} \delta_{\mathbf{k}_{\parallel}, \mathbf{k}'_{\parallel} \pm \mathbf{q}} \delta(\epsilon_{\mathbf{k}'_{\parallel}} - \epsilon_{\mathbf{k}_{\parallel}} \pm \hbar \omega_{\text{LO}}), \quad (1)$$

where N is the phonon distribution function at temperature T and is defined by $N = [\exp(\hbar \omega_{\text{LO}} / k_B T) - 1]^{-1}$; e is the electronic charge, ϵ_s and ϵ_{∞} are, respectively, the static and high frequency dielectric constants of the quantum well material (GaN), while V_0 is the large volume. The form factor $G(q_z)$ appropriate for a square quantum well of width L is explicitly given by¹⁵

$$G(q_z) = \frac{\pi^2}{(q_z L / 2)} \frac{\sin(q_z L / 2)}{[\pi^2 - (q_z L / 2)^2]}. \quad (2)$$

The total intrasubband scattering rate for an energy $\epsilon_{\mathbf{k}_{\parallel}}$ follows from Eq. (1) by summation over \mathbf{k}'_{\parallel} and \mathbf{q} and can be written as the sum of contributions from absorption (-) and emission (+) processes as follows:

$$\Gamma_{2\text{D}}(\epsilon_{\mathbf{k}_{\parallel}}) = \frac{1}{Z \epsilon_{\mathbf{k}_{\parallel}}^{1/2}} (I_- + I_+), \quad Z = \frac{8 \pi^2 \sqrt{2} \hbar \epsilon_0}{e^2 \omega_{\text{LO}} \sqrt{m^*}} \left(\frac{1}{\epsilon_{\infty}} - \frac{1}{\epsilon_s} \right)^{-1}, \quad (3)$$

where I_{\pm} are given by the integrals

$$I_{\pm} = \left(N + \frac{1}{2} \pm \frac{1}{2} \right) \theta(\epsilon_{\mathbf{k}_{\parallel}} - \frac{1}{2} \hbar \omega_{\text{LO}} \mp \frac{1}{2} \hbar \omega_{\text{LO}}) \times \int_{q_1^{\pm}}^{q_2^{\pm}} dq_{\parallel} \frac{2 \mathcal{F}(q_{\parallel})}{\left[4 - \left(\frac{k_{\parallel} \omega_{\text{LO}} \pm q_{\parallel}}{q_{\parallel} \epsilon_{\mathbf{k}_{\parallel}} \pm k_{\parallel}} \right)^2 \right]^{1/2}}, \quad (4)$$

where $\mathcal{F}(q_{\parallel})$ is given by

$$\mathcal{F}(q_{\parallel}) = \int_{-\infty}^{\infty} \frac{|G(q_z)|^2}{q_{\parallel}^2 + q_z^2} dq_z = \frac{8 \pi}{q_{\parallel} [4 \pi^2 + q_{\parallel}^2 d^2]} \left\{ \frac{\pi^2}{q_{\parallel} d} + \frac{3 q_{\parallel} d}{8} + \frac{4 \pi^4}{q_{\parallel}^2 d^2} \left(\frac{e^{-q_{\parallel} d} - 1}{4 \pi^2 + q_{\parallel}^2 d^2} \right) \right\}. \quad (5)$$

θ is the unit step function and the limits of the q_{\parallel} integrations are defined by

$$q_1^{\pm} = \pm k_{\parallel} \mp \left\{ k_{\parallel}^2 \mp \frac{2 m^* \omega_{\text{LO}}}{\hbar} \right\}^{1/2}, \quad q_2^{\pm} = k_{\parallel} + \left\{ k_{\parallel}^2 \mp \frac{2 m^* \omega_{\text{LO}}}{\hbar} \right\}^{1/2}. \quad (6)$$

III. SOLUTION OF THE BOLTZMANN EQUATION

A. The ladder technique

Our aim is to evaluate the PO phonon-limited low-field mobility of the 2D electron system subject to an electric field \mathbf{E} parallel to the quantum well planes. Previous treatments have dealt with mobility calculations in a number of ways, notably the variational method,¹⁶⁻¹⁹ the iteration method,²⁰ the matrix method,²¹ the Monte Carlo method,²²⁻²⁴ and methods dealing with standard and drifted distribution functions.^{25,26} In this paper we employ an exact method in which we solve the linearized Boltzmann equation following a ladder technique similar to that used by Delves.²⁷ The ladder technique is described at length by Fletcher and Butcher²⁸ and has recently been used by Ridley.²⁹ The distribution function of this electron system is taken to have the following form:

$$f(\mathbf{k}_{\parallel}) = f_0(\epsilon) + \left(\frac{\partial f_0(\epsilon)}{\partial \epsilon} \right) \mathbf{\Phi}(\mathbf{k}_{\parallel}) \cdot \mathbf{E}, \quad (7)$$

where $f_0(\epsilon)$ is the equilibrium Fermi-Dirac distribution function (low-electric-field approximation)

$$f_0(\epsilon) = \frac{1}{\exp(\epsilon - \epsilon_F) / k_B T + 1} \quad (8)$$

and we have dropped the subscript \mathbf{k}_{\parallel} in ϵ for ease of notation. The vector function $\mathbf{\Phi}$ is defined by solving the linearized Boltzmann equation

$$-\left(\frac{e \hbar}{m^*} \right) \mathbf{E} \cdot \mathbf{k}_{\parallel} \frac{\partial f_0}{\partial \epsilon} = \sum_{\mathbf{q}} \sum_{\mathbf{k}'_{\parallel}} \{ W_{\mathbf{k}'_{\parallel}, \mathbf{k}_{\parallel}, \mathbf{q}} f(\mathbf{k}'_{\parallel}) [1 - f(\mathbf{k}_{\parallel})] - W_{\mathbf{k}_{\parallel}, \mathbf{k}'_{\parallel}, \mathbf{q}} f(\mathbf{k}_{\parallel}) [1 - f(\mathbf{k}'_{\parallel})] \}, \quad (9)$$

where, on the right-hand side of this equation, $W_{\mathbf{k}_{\parallel}, \mathbf{k}'_{\parallel}, \mathbf{q}}$ stands for the scattering probability due to interaction with the polar-optical phonons and is defined in Eq. (1). The summand indicates that we have taken account of both processes

of transition into the state \mathbf{k}_{\parallel} and out of it, weighted by the probabilities of the electron states being empty or full. Clearly in conditions of statistical equilibrium, the electron flux in the transition $\mathbf{k}_{\parallel} \rightarrow \mathbf{k}'_{\parallel}$ must balance the reverse flux in the transition $\mathbf{k}'_{\parallel} \rightarrow \mathbf{k}_{\parallel}$ and so we have

$$W_{\mathbf{k}'_{\parallel}, \mathbf{k}_{\parallel}, q} f_0(\mathbf{k}'_{\parallel}) [1 - f_0(\mathbf{k}_{\parallel})] = W_{\mathbf{k}_{\parallel}, \mathbf{k}'_{\parallel}, q} f_0(\mathbf{k}_{\parallel}) [1 - f_0(\mathbf{k}'_{\parallel})]. \quad (10)$$

The main problem in solving the Boltzmann equation (9) is that it is not possible here to exploit the usual relaxation time approximation. This is due to the strong inelastic nature of the electron-PO-phonon interaction. As a result of this Eq. (9) should be treated as an algebraic difference equation in which the unknown energy function depends on three different arguments ϵ , $\epsilon + \hbar \omega_{\text{LO}}$, and $\epsilon - \hbar \omega_{\text{LO}}$.

The initial steps towards obtaining the solution involve substituting for the perturbed distribution function $f(\mathbf{k}_{\parallel})$ from Eq. (7) on the right-hand-side of Eq. (9), and retaining terms up to the first order in \mathbf{E} . We then identify the vector function Φ as the term proportional to \mathbf{k}_{\parallel} . We write

$$\Phi(\mathbf{k}_{\parallel}) = \frac{e\hbar}{m^*} \tau(\epsilon) \mathbf{k}_{\parallel}, \quad (11)$$

where $\tau(\epsilon)$ is an *effective* momentum relaxation time to be determined. The next steps involve substituting for the transition probability $W_{\mathbf{k}_{\parallel}, \mathbf{k}'_{\parallel}, q}$ from Eq. (1), converting the summation into an integration and finally eliminating the electric field. We obtain a difference equation which can be written in the following form:

$$Z\epsilon^{3/2} = A(\epsilon)\tau(\epsilon + \hbar\omega_{\text{LO}}) + B(\epsilon)\tau(\epsilon) + C(\epsilon)\tau(\epsilon - \hbar\omega_{\text{LO}}), \quad (12)$$

where the functions A, B, C are defined as follows:

$$A(\epsilon) = -(N+1) \frac{f_0(\epsilon + \hbar\omega_{\text{LO}})}{f_0(\epsilon)} I_{A-}, \quad (13)$$

$$B(\epsilon) = \left[(N+1) \frac{f_0(\epsilon + \hbar\omega_{\text{LO}})}{f_0(\epsilon)} I_{B-} + N \frac{f_0(\epsilon - \hbar\omega_{\text{LO}})}{f_0(\epsilon)} I_{B+} \right], \quad (14)$$

$$C(\epsilon) = -N \frac{f_0(\epsilon - \hbar\omega_{\text{LO}})}{f_0(\epsilon)} I_{A+} \quad (15)$$

in which the integrals $I_{A\pm}$ and $I_{B\pm}$ are given by

$$I_{A\pm} = \int_{q_1^{\pm}}^{q_2^{\pm}} dq_{\parallel} \frac{\mathcal{F}(q_{\parallel}) (2\epsilon \mp \hbar\omega_{\text{LO}} - \hbar^2 q_{\parallel}^2 / 2m^*)}{[4 - (k_{\parallel} \hbar\omega_{\text{LO}} / q_{\parallel} \epsilon \pm q_{\parallel} / k_{\parallel})^2]^{1/2}} \times \theta(\epsilon - \frac{1}{2} \hbar\omega_{\text{LO}} \mp \frac{1}{2} \hbar\omega_{\text{LO}}), \quad (16)$$

$$I_{B\pm} = \int_{q_1^{\pm}}^{q_2^{\pm}} dq_{\parallel} \frac{2\epsilon \mathcal{F}(q_{\parallel})}{[4 - (k_{\parallel} \hbar\omega_{\text{LO}} / q_{\parallel} \epsilon \pm q_{\parallel} / k_{\parallel})^2]^{1/2}} \times \theta(\epsilon - \frac{1}{2} \hbar\omega_{\text{LO}} \mp \frac{1}{2} \hbar\omega_{\text{LO}}). \quad (17)$$

It is seen from Eq. (12) that if we can obtain a good estimate of $\tau(\epsilon)$ in the first energy interval $0 < \epsilon < \hbar\omega_{\text{LO}}$, then it is a simple matter to generate $\tau(\epsilon)$ for any ϵ . However, any estimates of $\tau(\epsilon)$ in the first interval must be extremely accurate, otherwise even small deviations quickly become significant. The ladder technique adopted here involves writing Eq. (12) as an infinite set of equations, one for each of the energy intervals as follows:

$$\begin{aligned} A(\epsilon_0)\tau_1 + B(\epsilon_0)\tau_0 &= Z\epsilon_0^{3/2}, \\ A(\epsilon_1)\tau_2 + B(\epsilon_1)\tau_1 + C(\epsilon_1)\tau_0 &= Z\epsilon_1^{3/2}, \\ &\dots, \\ A(\epsilon_m)\tau_{m+1} + B(\epsilon_m)\tau_m + C(\epsilon_m)\tau_{m-1} &= Z\epsilon_m^{3/2}, \\ &\dots, \end{aligned} \quad (18)$$

where $\epsilon_n = \epsilon' + n\hbar\omega_{\text{LO}}$ with $0 < \epsilon' < \hbar\omega_{\text{LO}}$ and $\tau_n = \tau(\epsilon_n)$. We get successive equations by assigning integer $n \geq 0$ and setting $\tau_{-1} = 0$. The series of equations indicate that τ_0 is determined by in-scattering events from the state $\epsilon' + \hbar\omega_{\text{LO}}$ and out-scattering from ϵ' , whereas τ_m is determined by in-scattering events from the states $\epsilon' + (m \pm 1)\hbar\omega_{\text{LO}}$ and out-scattering from $\epsilon' + m\hbar\omega_{\text{LO}}$. Thus, in principle, τ_0 depends on $\tau_1, \tau_2, \dots, \tau_m, \dots$, and so on through all the in-scattering terms. The procedure involves truncating the set of equations at the n th equation, and we are left to solve n equations for $(n+1)$ unknowns. The additional condition which is needed to obtain a solution is provided by application of a boundary condition. Clearly we must have $\tau(\epsilon) = 0$ for $\epsilon < 0$. As for the upper limit, we note that Grigor'ev *et al.*²¹ and also Fletcher and Butcher²⁸ make use of the fact that for $\epsilon \gg \hbar\omega_{\text{LO}}$ we may write $\tau(\epsilon \pm \hbar\omega_{\text{LO}}) \approx \tau(\epsilon)$. Hence the upper limit may be written as

$$\tau(\epsilon) \rightarrow \frac{Z\epsilon^{3/2}}{A(\epsilon) + B(\epsilon) + C(\epsilon)}, \quad \epsilon \rightarrow \infty. \quad (19)$$

This is the condition adopted in this paper. The solution of the set of equations, together with Eq. (19), can be found using matrix inversion techniques. For a given ϵ a trial value of n is first used in the computations and then gradually increased to achieve a sufficiently accurate value of $\tau(\epsilon_n)$. The procedure is then repeated for different ϵ to produce values of $\tau(\epsilon)$ covering the entire energy range. The error in the final effective relaxation time $\tau(\epsilon)$ is small for small ϵ , but is liable to increase as ϵ increases. Fortunately this error should not affect the accuracy of any transport coefficients thus derived, as the contribution of high-energy electrons to the transport coefficients is small because of their small number.

B. The low-energy approximation

This is a particular approximation that is suitable for conditions in which $k_B T < \hbar\omega_{\text{LO}}$ and $\epsilon_F < \hbar\omega_{\text{LO}}$, which are consistent with electrons having energy no higher than $2\hbar\omega_{\text{LO}}$.

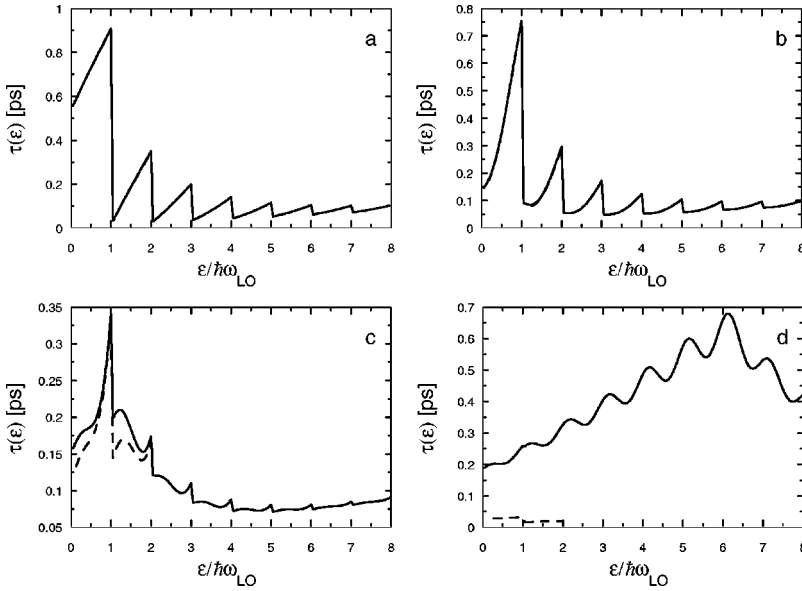


FIG. 2. Variation with ϵ of the momentum relaxation time $\tau(\epsilon)$ (solid curve), evaluated for a fixed well width $L=3$ nm and fixed electron density and temperature using the exact ladder method described in Sec. III A. Also shown spanning the first two energy intervals are the corresponding results emerging from the low-energy approximation (dashed curve) of Sec. III B [the curves coincide (a) and (b)]. The values of the electron densities in these figures are as follows: (a), $n_0=10^{10}$ cm $^{-2}$; (b), $n_0=5.0\times 10^{12}$ cm $^{-2}$; (c), $n_0=10^{13}$ cm $^{-2}$; and (d), $n_0=5.0\times 10^{13}$ cm $^{-2}$. The temperature was fixed at 300 K throughout. The relevant GaN parameters are $\hbar\omega_{LO}=92.8$ meV; $m^*=0.21m_e$; $\epsilon_s=9.5$ and $\epsilon_\infty=5.37$.

Under such conditions, we need only consider out of the set (18) the first two equations with $m=0,1$, ignoring terms involving τ_2 ,

$$A(\epsilon_0)\tau_1 + B(\epsilon_0)\tau_0 = Z\epsilon_0^{3/2}, \quad (20)$$

$$A(\epsilon_1)\tau_2 + B(\epsilon_1)\tau_1 + C(\epsilon_1)\tau_0 = Z\epsilon_1^{3/2}, \quad (21)$$

which can be solved to yield

$$\tau_0 = Z \frac{B(\epsilon_1)\epsilon_0^{3/2} - A(\epsilon_0)\epsilon_1^{3/2}}{B(\epsilon_0)B(\epsilon_1) - A(\epsilon_0)C(\epsilon_1)}, \quad (22)$$

$$\tau_1 = Z \frac{B(\epsilon_0)\epsilon_1^{3/2} - C(\epsilon_1)\epsilon_0^{3/2}}{B(\epsilon_0)B(\epsilon_1) - A(\epsilon_0)C(\epsilon_1)}.$$

We call this the low-energy approximation, which is similar to that of Grigor'ev *et al.*²¹ except that we include two intervals of $\hbar\omega_{LO}$ rather than one. The validity of this approximation depends on the temperature and the degeneracy of the electron system and it would be instructive to examine its accuracy relative to the exact ladder method when we consider the variation with the parameters.

C. Results for the momentum relaxation time

Figures 2(a) to 2(d) show the variation with ϵ of the momentum relaxation time $\tau(\epsilon)$, evaluated at room temperature $T=300$ K for a fixed well width $L=3$ nm and fixed electron density using the exact ladder method described in Sec. III A. The values of the electron densities in these figures are as follows: Fig. 2(a), $n_0=10^{10}$ cm $^{-2}$ ($\epsilon_F=-140$ meV); Fig. 2(b), $n_0=5.0\times 10^{12}$ cm $^{-2}$ ($\epsilon_F=54$ meV); Fig. 2(c), $n_0=10^{13}$ cm $^{-2}$ ($\epsilon_F=114$ meV); and Fig. 2(d), $n_0=5.0\times 10^{13}$ cm $^{-2}$ ($\epsilon_F=569$ meV). A common feature of these results is that $\tau(\epsilon)$ exhibits steps at all integer multiples of

$\hbar\omega_{LO}$. The first step arises due to the sudden onset of emission when the electron energy becomes equal to $\hbar\omega_{LO}$. The subsequent steps arise at higher multiples of $\hbar\omega_{LO}$ due to their link to the variations in the first energy interval $0 < \epsilon < \hbar\omega_{LO}$ at each absorption and emission of a phonon. It is also seen that for $\epsilon_F < \hbar\omega_{LO}$, the momentum relaxation time τ decreases with increasing density, with smaller and less sharper steps. The trend is such that at higher density the steps would disappear and would be replaced by a smooth curve, exhibiting a maximum at the Fermi energy. Also shown spanning the first two energy intervals in Figs. 2(a) to 2(d) are the corresponding results emerging from the low-energy approximation of Sec. III B. Clearly this approximation provides good representations of the results for the relatively small densities in Figs. 2(a) and 2(b), but substantial deviations from the exact results are seen at the higher densities in Figs. 2(c) and 2(d). This feature would have to be borne in mind when calculating the low-field mobility at high electron densities.

Figures 3(a) to 3(c) show the variations of the momentum relaxation time for fixed $\epsilon = \hbar\omega_{LO}/2$. Figure 3(a) displays the variations of $\tau(\hbar\omega_{LO}/2)$ with the well width for a fixed electron density $n_0=5.0\times 10^{12}$ cm $^{-1}$. At this low energy $\epsilon = \hbar\omega_{LO}/2$ and at low density the approximate theory in Sec. III B is seen to provide a good representation of the exact results spanning the range of well widths shown in the figure. Figure 3(b) shows the variations of $\tau(\hbar\omega_{LO}/2)$ with electron density for a fixed well width $L=3$ nm. Once again for $\epsilon = \hbar\omega_{LO}/2$ the low-energy approximation provides a good representation of the results at low and moderately high densities. At very high densities, however, the low-energy approximation diverges widely from the exact results. Finally the variations of $\tau(\hbar\omega_{LO}/2)$ with temperature are displayed in Fig. 3(c) for a fixed electron density $n_0=5.0\times 10^{12}$ cm $^{-2}$ and a fixed well width $L=3$ nm.

IV. EVALUATION OF THE MOBILITY

The mobility μ in two dimensions is related to $\tau(\epsilon)$ as follows:¹⁵

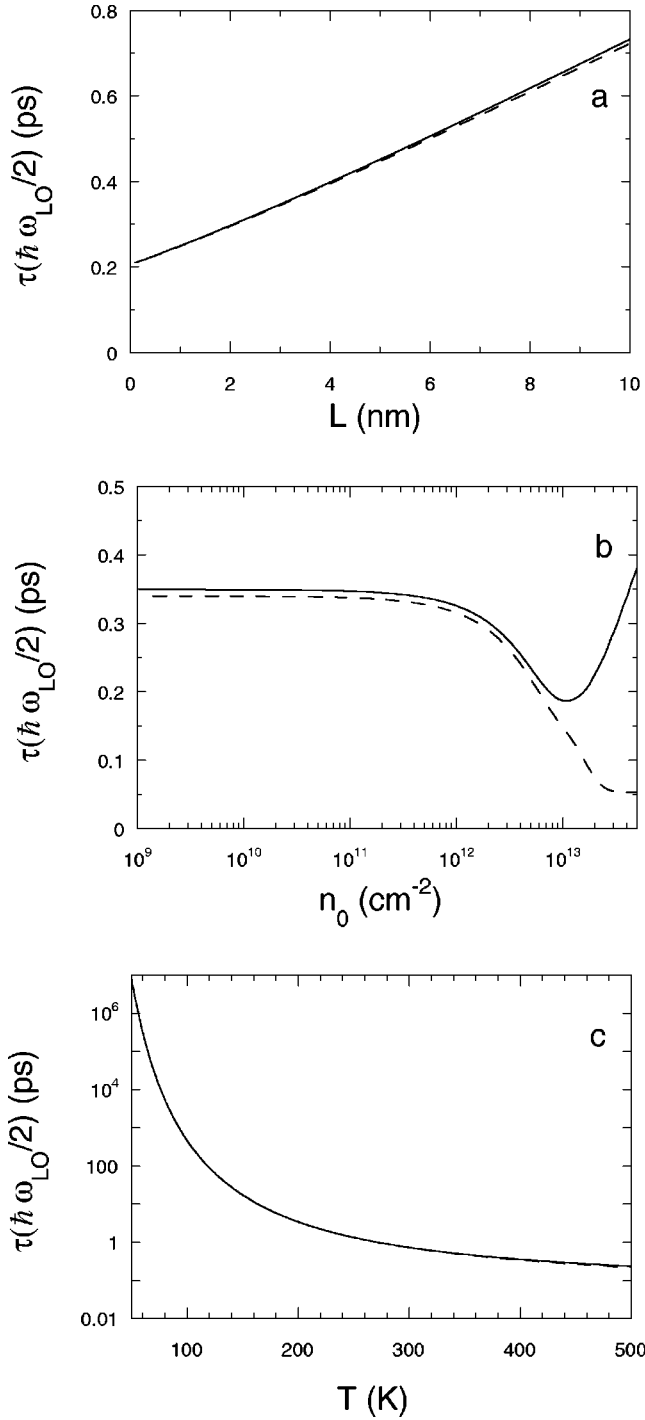


FIG. 3. Variations of the momentum relaxation time for a fixed $\epsilon = \hbar\omega_{LO}/2$: (a) variations of $\tau(\hbar\omega_{LO}/2)$ with the well width for a fixed temperature $T=300$ K and a fixed electron density $n_0=5.0 \times 10^{12}$ cm^{-2} ; (b) variations of $\tau(\hbar\omega_{LO}/2)$ with electron density for a fixed well width $L=3$ nm and a fixed temperature $T=300$ K; (c) variations of $\tau(\hbar\omega_{LO}/2)$ with temperature for a fixed electron density $n_0=5.0 \times 10^{12}$ cm^{-2} and a fixed well width $L=3$ nm. The full curves represent the results using the exact ladder method of Sec. III A and the dashed curves are those emerging from the low-energy approximation of Sec. III B [the curves coincide in (c)]. The parameters used are the same as those quoted in Fig. 2.

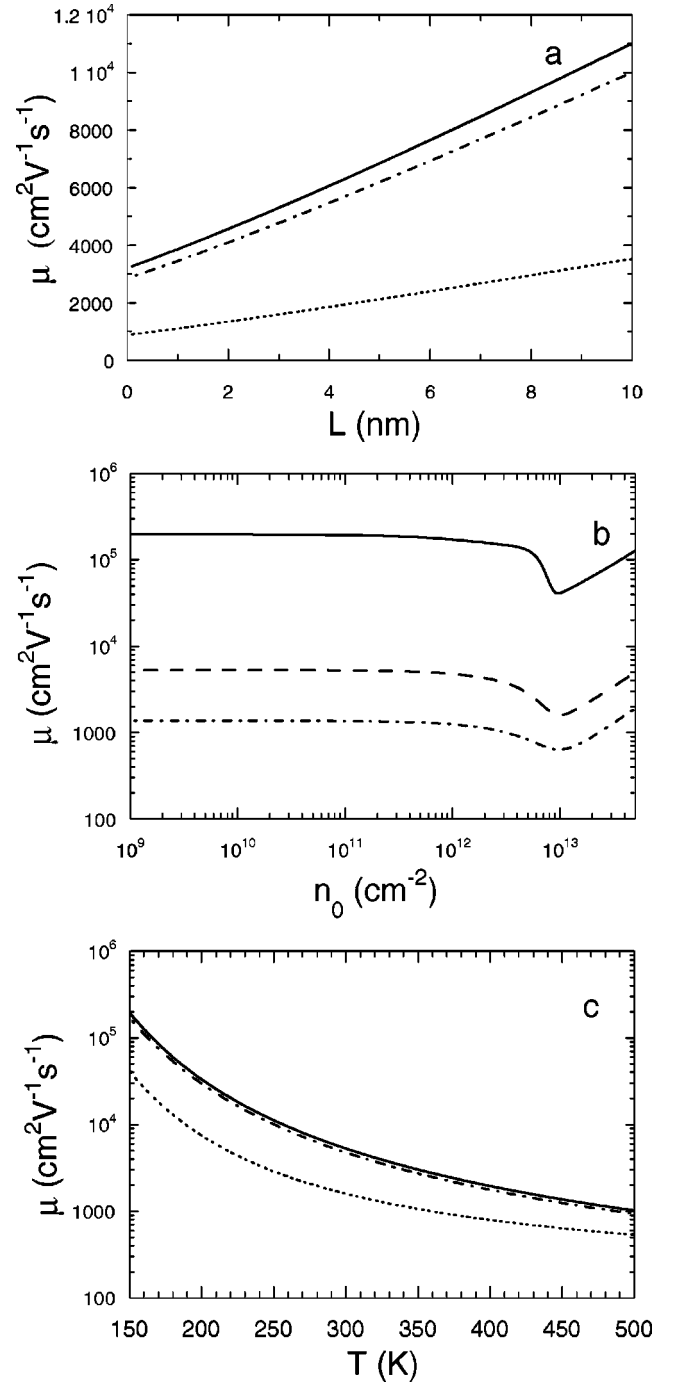


FIG. 4. (a) Variation of the mobility with the GaN/AlN quantum well width for three different values of the electron density $n_0 = 10^{10}$ cm^{-2} (solid curve); $n_0 = 10^{12}$ cm^{-2} (dot-dashed curve); $n_0 = 10^{13}$ cm^{-2} (dotted curve). (b) Variation of the mobility with the two-dimensional electron density in a GaN/AlN quantum well of width $L=3$ nm. The different curves correspond to different temperatures: $T=150$ K (solid curve); $T=300$ K (dashed curve); and $T=450$ K (dash-dot curve); (c) variation of the mobility in a GaN/AlN quantum well of width $L=3$ nm as a function of temperature for three different values of electron density: $n_0 = 10^{10}$ cm^{-2} (solid curve); $n_0 = 10^{12}$ cm^{-2} (dot-dashed curve); $n_0 = 10^{13}$ cm^{-2} (dotted curve). The parameters used are the same as those quoted in Fig. 2.

$$\mu = \frac{e}{\pi \hbar^2 n_0 k_B T} \int_0^\infty \tau(\epsilon) f_0(\epsilon) [1 - f_0(\epsilon)] \epsilon d\epsilon. \quad (23)$$

The results for the mobility are based on this equation and require numerical integration with input from the methods described in Secs. III A and III B for the evaluation of $\tau(\epsilon)$. The variation of the mobility with the parameters are shown in Figs. 4(a)–4(c). Figure 4(a) displays its variation with the GaN/AlN quantum well width for different values of the electron density. The curves exhibit a general trend of increasing mobility with increasing quantum well width. This is consistent with a corresponding increase of the electron density of states with increasing well width. In Fig. 4(b) the variation of the mobility with the two-dimensional electron density is shown for a GaN/AlN quantum well of width $L = 3$ nm. The different curves correspond to different temperatures and it is seen that the curves are practically flat for a wide range of density, but each curve exhibits a clear minimum at a characteristic density. It can be seen that this is consistent with the behavior of the momentum relaxation time in Fig. 3(b). Finally, in Fig. 4(c) the mobility in a GaN/AlN quantum well of width $L = 3$ nm is presented as a function of the temperature for different values of electron density. There is a general trend of a decrease of the mobility with increasing temperature, and this feature has its origin mainly in the distribution functions, which lead to a decrease of the momentum relaxation rate and hence the mobility with increasing temperature. The dependence of the mobility on electron density as shown in Fig. 4(b) exhibits a pronounced minimum at a characteristic density. We have checked that this feature coincides with the condition $\epsilon_F \approx \hbar \omega_{LO}$. This corresponds to an increase in the emission rate and a decrease in the momentum relaxation time as in Fig. 3(b). For GaN quantum wells the drop in mobility in this region of density should, in principle, be experimentally accessible.

V. COMMENTS AND CONCLUSIONS

We have studied electron transport in square GaN/AlN quantum wells in which the electron system is degenerate, systematizing the procedure leading to the evaluation of the momentum relaxation time, and this enabled calculations of the mobility to be carried out. A prominent feature of the results for the momentum relaxation time $\tau(\epsilon)$ are the steps

at integer multiples of $\hbar \omega_{LO}$. The first step arises due to the sudden onset of emission when the electron energy becomes equal to $\hbar \omega_{LO}$. The subsequent steps arise at higher multiples of $\hbar \omega_{LO}$ due to their link to the variations in the first energy interval $0 < \epsilon < \hbar \omega_{LO}$ at each absorption and emission of a phonon. Another feature is that for $\epsilon_F < \hbar \omega_{LO}$ the momentum relaxation time τ decreases with increasing density, with smaller and less sharper steps as the density increases. The trend is such that at higher densities the steps would disappear and would be replaced by a smooth curve exhibiting a maximum at the Fermi energy.

We have highlighted the low-energy approximation in this context and showed that at low energies $\epsilon \leq 2\hbar \omega_{LO}$ this approximation provides a good representation of the exact results spanning a fairly wide range of well widths and for low to moderate electron densities. At very high densities, however, the low-energy approximation diverges widely from the exact results. Finally we have drawn attention to the existence of a minimum in the variations of the mobility with electron density and suggested that for GaN quantum wells this should, in principle, be experimentally measurable.

The work carried out here needs to be extended to take account of different regimes of approximations. First, at high densities screening effects must be explicitly included in the formalism, as well as the coupled mode effects at densities for which the plasma frequency becomes comparable to the PO phonon frequency. Second, the one-subband model is expected to be inadequate as soon as the Fermi energy becomes comparable to the energy separation between the lowest two quantum well subbands. The two-subband problem using the ladder technique would be intractable, however, as would be the one-subband problem involving two phonon-plasmon coupled modes of different frequencies. Finally, the allied problem of electron transport in a triangular quantum well needs to be addressed using the ladder technique, with particular emphasis on the density dependence of the effective well width.³⁰ These regimes will not be considered any further here.

ACKNOWLEDGMENTS

The authors wish to thank the U.K. Engineering and Physical Sciences Research Council (EPSRC) for support through Grant No. GR/L56725, under which this work was carried out.

¹S. Nakamura and G. Fasol, *The Blue Laser Diode: GaN-Based Light Emitters and Lasers* (Springer-Verlag, Berlin, 1997).

²For recent developments see *GaN and Related Alloys*, edited by S.J. Pearton, C. Kuo, A.F. Wright, and T. Uenoyama, MRS Symposium Proceedings Mater. Res. Soc. Symp. Proc. **537**, Materials Research Society, Warrendale, 1999.

³C. Mailhiot and D.L. Smith, *Rev. Mod. Phys.* **62**, 173 (1990).

⁴D.L. Smith, *Solid State Commun.* **57**, 919 (1986).

⁵F. Bernardini and V. Fiorentini, *Phys. Rev. B* **56**, R10 024 (1997).

⁶F.D. Sala, A.D. Carlo, P. Luigi, F. Bernardini, V. Fiorentini, R.

Scholc, and J.-M. Janco, *Appl. Phys. Lett.* **74**, 3426 (1998).

⁷E.S. Snow, B.V. Shanabrook, and D. Gammon, *Appl. Phys. Lett.* **56**, 758 (1990).

⁸R. Gaska, J.W. Yang, A. Osinsky, A.D. Bokhovski, and M.S. Shur, *Appl. Phys. Lett.* **73**, 3577 (1998); A.D. Bokhovski, R. Gaska, and M.S. Shur, *ibid.* **71**, 3674 (1997).

⁹O. Ambacher, J. Smart, J.R. Shealy, N.G. Weinman, K. Chu, M. Murohy, W.J. Schaff, L.F. Eastman, R. Dimitrov, L. Wittmer, M. Stutzman, W. Rieger, and J. Hilsenbeck, *J. Appl. Phys.* **85**, 3222 (1999).

- ¹⁰R. Gaska, J.W. Yang, A. Osinsky, Q. Chen, M.A. Khan, A.O. Orlov, G.L. Snider, and M.S. Shur, *Appl. Phys. Lett.* **72**, 707 (1998).
- ¹¹R. Oberhuber, G. Zandler, and P. Vogl, *Appl. Phys. Lett.* **73**, 818 (1998).
- ¹²R. Gaska, M. Shur, A.D. Bokhovski, A.O. Orlov, and G.L. Snider, *Appl. Phys. Lett.* **74**, 287 (1999).
- ¹³M. Babiker and N. Zakhleniuk, in *Hot Electrons in Semiconductors: Physics and Devices*, edited by N. Balkan (Clarendon, Oxford, 1998), Chap. 6.
- ¹⁴N. A. Zakhleniuk, C. R. Bennett, M. Babiker, and B. K. Ridley, in *III-V Nitride Semiconductors: Electrical, Structural, and Defect Properties*, edited by O. Manasreh (Elsevier, Amsterdam, 2000), Chap. XI.
- ¹⁵B. K. Ridley, *Electrons and Phonons in Semiconductor Multilayers* (Cambridge University Press, Cambridge, 1997).
- ¹⁶E.H. Sondheimer and D.J. Howarth, *Proc. R. Soc. London, Ser. A* **219**, 53 (1953).
- ¹⁷B.E. Lewis and E.H. Sondheimer, *Proc. R. Soc. London, Ser. A* **227**, 241 (1955).
- ¹⁸F. Garcia Moliner, *Phys. Rev.* **130**, 2290 (1963).
- ¹⁹H.E. Ehrenreich, *J. Phys. Chem. Solids* **9**, 129 (1959); *Phys. Rev.* **120**, 1951 (1960).
- ²⁰D.L. Rode, *Semicond. Semimetals* **10**, 1 (1975).
- ²¹N.N. Grigor'ev, I.M. Dykman, and P.M. Tomchuk, *Fiz. Tverd Tela (Leningrad)* **10**, 1058 (1968) [*Sov. Phys. Solid State* **10**, 837 (1968)].
- ²²M.A. Littlejohn, J.R. Hauser, and T.H. Glisson, *Appl. Phys. Lett.* **26**, 625 (1975).
- ²³B. Gelmont, K. Kim, and M. Shur, *J. Appl. Phys.* **74**, 1818 (1993).
- ²⁴I.H. Aguzman, J. Kolnik, K.F. Breenan, R. Wand, T.N. Fang, and P.P. Ruden, *J. Appl. Phys.* **80**, 4429 (1996).
- ²⁵B. Gelmont, M. Shur, and M.J. Stroschio, *J. Appl. Phys.* **77**, 657 (1995).
- ²⁶H. Callen, *Phys. Rev.* **76**, 1395 (1949).
- ²⁷R.T. Delves, *Proc. Phys. Soc. London* **73**, 572 (1959).
- ²⁸K. Fletcher and P.N. Butcher, *J. Phys. C* **5**, 212 (1972).
- ²⁹B.K. Ridley, *J. Phys.: Condens. Matter* **10**, 6717 (1998).
- ³⁰B.K. Ridley, B.E. Foutz, and L.E. Eastman, *Phys. Rev. B* **61**, 16 821 (2000).